

This is the author's version of a work that was accepted for publication in Atmospheric environment (Ed. Elsevier). Changes resulting from the publishing process, such as peer review, editing, corrections, structural formatting, and other quality control mechanisms may not be reflected in this document. Changes may have been made to this work since it was submitted for publication. A definitive version was subsequently published in Izquierdo, R. et al. "Effects of teleconnection patterns on the atmospheric routes, precipitation and deposition amounts in the north-eastern Iberian Peninsula" in Atmospheric environment, vol. 89 (June 2014), p. 482-490.

DOI 10.1016/j.atmosenv.2014.02.057

Effects of teleconnection patterns on the atmospheric routes, precipitation and deposition amounts in the north-eastern Iberian Peninsula

Rebeca Izquierdo<sup>1</sup>, Marta Alarcón<sup>2</sup>, Laura Aguilhaume<sup>1</sup>, and Anna Àvila<sup>1\*</sup>

(1) CREA, Universitat Autònoma de Barcelona, Cerdanyola del Vallès 08193, Spain

(2) Departament de Física i Enginyeria Nuclear, Universitat Politècnica de Catalunya, c/ Urgell 187, 08036 Barcelona, Spain

\*Corresponding author:

[anna.avila@uab.cat](mailto:anna.avila@uab.cat)

Tel: +34 93 581 4669

Fax: +34 93 581 4151

25 Abstract

26 The North Atlantic Oscillation (NAO) has been identified as one of the atmospheric patterns  
27 which mostly influence the temporal evolution of precipitation and temperature in the  
28 Mediterranean area. Recently, the Western Mediterranean Oscillation (WeMO) has also been  
29 proposed to describe the precipitation variability in the eastern Iberian Peninsula. This paper  
30 examines whether the chemical signature and/or the chemical deposition amounts recorded  
31 over NE Iberian Peninsula are influenced by these climatic variability patterns. Results show a  
32 more relevant role of the WeMO compared to NAO in the deposition of either marine ( $\text{Cl}^-$ ,  $\text{Na}^+$ ,  
33  $\text{Mg}^{2+}$ ) or anthropogenic pollutants ( $\text{H}^+$ ,  $\text{NH}_4^+$ ,  $\text{NO}_3^-$  and  $\text{SO}_4^{2-}$ ). A cluster classification of  
34 provenances indicated that in winter (December to March) fast Atlantic air flows correspond to  
35 positive WeMO indices, while negative WeMOi are associated to Northeastern and  
36 Southwestern circulations. The negative phase of WeMO causes the entry of air masses from  
37 the Mediterranean into the Iberian Peninsula, that are enriched with marine ions and ions of  
38 anthropogenic origin ( $\text{NH}_4^+$ ,  $\text{NO}_3^-$  and  $\text{SO}_4^{2-}$ ). For these later, this suggests the advection over  
39 the Mediterranean of polluted air masses from southern Europe and the scavenging and  
40 deposition of this pollution by precipitation during the WeMO negative phases. This will carry  
41 transboundary pollutants to the NE Iberian Peninsula. However, local pollutants may also  
42 contribute, as precipitation events from the Mediterranean and the Atlantic (associated to both  
43 WeMO phases) may incorporate emissions that accumulate locally during the winter  
44 anticyclonic episodes typical of the region.

45

46

47 Key words: West Mediterranean, precipitation chemistry, deposition, back-trajectories, NAO,  
48 WeMO

49

50

51

52

53

54 WeMO index better describes winter precipitation in the NE Iberian Peninsula than NAO

55 Element deposition was correlated with NAO and WeMO depending on air provenance

56 Few studies have analyzed the relationship rain chemistry vs. NAO and WeMO

57

58

59

60

61

62

63 1. Introduction

64 The chemical composition of precipitation is strongly influenced by the predominant  
65 atmospheric transport patterns, which affect the scavenging of pollutants depending on the  
66 pollution climate encountered. Also, the precipitation amount is important as it influences the  
67 dilution and amount of pollutants. The Iberian Peninsula (IP) is located in the south-western  
68 corner of the European continent, with the Atlantic Ocean to the west and the Mediterranean to  
69 the east, the industrialized Europe to the north and the arid Africa to the south, thus it is in a  
70 crossroads influenced by pollutant sources differing strongly in strength and character, which  
71 will affect the precipitation chemistry. The levels of atmospheric particulate matter (PM) in this  
72 area and its chemical composition has been shown to depend on the origin of air masses  
73 (Pérez et al. 2008; Querol et al. 2009; Pey et al. 2009, 2010; Cusack et al. 2012) and the  
74 chemical composition of precipitation as well (Àvila and Alarcón 1999, 2003; Izquierdo et al.  
75 2012). African events have been found to be related with the specific position of cyclonic lows in  
76 the western or southern flank of the IP or the permanence of high pressures over north Africa in  
77 summer (Escudero et al. 2005, 2011). A higher contribution of African precipitation events for  
78 particular years significantly affects the acidity/alkalinity balance of precipitation and the  
79 contribution of crustal components (Àvila et al. 1997, 2007; Àvila and Rodà 2002; Pulido-Villena  
80 et al. 2006; Morales-Baquero et al. 2013). Furthermore, the region is subject to a large load of  
81 anthropogenic emissions from the intense activity of large cities such as Marseille, Barcelona  
82 and Tarragona and their industrial surroundings and of the heavy traffic along the eastern coast  
83 of IP. The pollutant climate in this area is further modulated by a marked seasonality. In winter,  
84 the frequent entry of Atlantic relatively clean air fluxes induces the replacement of air masses,  
85 thus reducing the levels of atmospheric pollutants that may have accumulated during periods of  
86 anticyclonic stability (Rodríguez et al. 2003; Escudero et al. 2007). In contrast, the synoptic  
87 scenario in summer is characterized by very weak pressure gradients in the western  
88 Mediterranean which produce local circulations enhancing the regional accumulation of  
89 pollutants (Millán et al. 1991, 1997; Rodríguez et al. 2003).

90 In the Mediterranean area, a year to year variability in the amount of precipitation (Xoplaki 2002;  
91 Lionello et al. 2006; Mariotti and Dell'Aquila 2012) and dust transport (Moulin et al. 1997;  
92 Ginoux et al. 2004; Pey et al. 2013) has been related to the atmosphere-ocean interaction  
93 defined as the North Atlantic Oscillation (NAO). The NAO strongly influences the atmospheric  
94 circulation and the hydrological cycle in the Northern hemisphere (Hurrell 1995; Wallace 2000;  
95 Hurrell et al. 2004; Hurrell and Deser 2010). An intensification of NAO (producing more westerly  
96 winds across the North Atlantic and into Eurasia) has been observed over the past few decades  
97 (Hurrell 1995). This intensification would bring an increase in precipitation in mid-latitude zones  
98 in Europe. Although many models suggest that such a change might be the result of  
99 anthropogenic greenhouse warming (Carnell and Senior, 2002; Zhang et al. 2007; Min et al.  
100 2011), most models seem to underestimate the magnitude of this circulation change in central

101 Europe (Gillett et al. 2005). In the Mediterranean, Barkhordarian et al. (2013) indicate that  
102 changes in atmospheric greenhouse gas and sulphate concentrations are not the dominant  
103 forcing process affecting precipitation changes in this area. Additional anthropogenic forcing  
104 agents potentially have a larger effect on regional scale precipitation. The emission of aerosols  
105 related to traffic and industry and/or forcing from land-use changes such as deforestation are  
106 missing in current climate models and need to be incorporated.

107 Recently, the Western Mediterranean Oscillation (WeMO) climatic variability has been proposed  
108 to describe the synoptic framework of the western Mediterranean basin (Martín-Vide and López-  
109 Bustins, 2006). The WeMO index is calculated as the difference between the standardized  
110 surface pressure values recorded at Padua (45.40°N, 11.48°E) in northern Italy, an area with a  
111 relatively high barometric variability due to the influence of the central European anticyclone,  
112 and San Fernando (Cádiz) (36.28°N, 6.12°W) in south-western Spain, an area often influenced  
113 by the Azores anticyclone (Fig.1). This regional pattern strongly determines the variability of  
114 rainfall in the eastern façade of the IP (Martín-Vide and López-Bustins, 2006; González-Hidalgo  
115 et al. 2009). As in most of the variability patterns of the Northern Hemisphere, WeMO shows its  
116 most relevant dynamics during the winter (Martín-Vide and López-Bustins 2006). The WeMO  
117 positive phase has been shown to trigger air masses from the Atlantic to move into the IP, while  
118 its negative phase is associated to flows from the Mediterranean (Martín-Vide and López-  
119 Bustins 2006; López-Bustins et al. 2008). Thus, it can be foreseen that part of the precipitation  
120 variability and precipitation chemical signature in Northeastern Spain may be related to the  
121 WeMO pattern. The effects of the WeMO on precipitation amounts in NE Spain has been  
122 recently explored (López-Bustins et al. 2008, González-Hidalgo et al. 2009), but to our  
123 knowledge, no studies have been focused on the analysis of its influence on the precipitation  
124 chemical composition.

125 We explore here whether the chemical signature and/or the chemical deposition amounts  
126 reaching a site in Catalonia (NE Iberian Peninsula) is influenced by these climatic variability  
127 patterns. This is studied by comparing winter bulk precipitation chemistry data at a locality in  
128 Catalonia (La Castanya) and the NAO and WeMO indexes for a long-time series of weekly  
129 precipitation chemical data from 1984 to 2012. Thus, this study covers a 3-decade period where  
130 changes in emissions have taken place in Europe in response to emission abatement strategies  
131 agreed under the Convention on Long-range Transboundary Air Pollution (UNECE, available at  
132 <http://www.unece.org/env/lrtap/>). The aim here is to discern the influence of the main circulation  
133 patterns as represented by NAO and WeMO on precipitation amounts and the chemical loads of  
134 precipitation.

135

136

137

## 138 2. Material and Methods

### 139 2.1. Study site

140 La Castanya station (LC, 41°46'N, 2°21'E, 700 m) is located in the Montseny mountains of the  
141 Pre-litoral Catalan Range. Long-term biogeochemical studies have been undertaken since the  
142 1970s in a forest plot close to the atmospheric sampling site (Rodà et al. 1999). The site is  
143 amidst extensive holm-oak (*Quercus ilex* L.) forests in the Montseny Natural Park, 40 km to the  
144 N-NE from Barcelona and 25 km from the Mediterranean coast (Fig.1). The climate in Montseny  
145 is meso-Mediterranean sub-humid, with high interannual precipitation variability (range: 503-  
146 1638 mm y<sup>-1</sup>, mean: 840 mm y<sup>-1</sup> at LC, from 1983-2009). Summer droughts are common and  
147 snow is sporadic. Mean air temperature was 9°C during the period 1983-2000 at LC.

### 148 2.2. Sampling and chemical analysis

149 We analyze here the precipitation chemistry in the period 1984-2012. Weekly samples were  
150 obtained with 4 or 2 bulk deposition collectors (consisting of a polyethylene funnel connected to  
151 a 10L bottle) located in a clearing within the holm oak forest. Bulk deposition samples were  
152 obtained from 1983 to 2001; wet-only deposition was also collected in parallel with bulk  
153 deposition for 2008-2012. In order to obtain an homogeneous data record, regressions between  
154 bulk and wet weekly data were used to estimate bulk deposition for the whole period and very  
155 strong correlations were obtained ( $R > 0.8$ ,  $p < 0.001$ ). Measurements here considered  
156 correspond to bulk deposition weekly samples. Further details can be found in Izquierdo and  
157 Àvila (2012) and Izquierdo et al. (2012). Samples were processed in the CREAM laboratory  
158 according to previously described protocols (Àvila 1996; Àvila and Rodà 2002). Conductivity,  
159 alkalinity and pH were measured in unfiltered samples within 48h of sampling. Samples were  
160 filtered through 0.45µm membrane filters and stored at -20°C. Ion chromatography was used to  
161 determine the concentrations of Na<sup>+</sup>, K<sup>+</sup>, Mg<sup>2+</sup>, Ca<sup>2+</sup>, NH<sub>4</sub><sup>+</sup>, Cl<sup>-</sup>, NO<sub>3</sub><sup>-</sup> and SO<sub>4</sub><sup>2-</sup>. Quality control  
162 included the repeated inclusion of certified samples and the checking of ratios (measured  
163 conductivity against the calculated conductivity and the sum of cations against the sum of  
164 anions) and samples were reanalyzed or discarded for differences > 20% (Àvila 1996; Àvila and  
165 Rodà 2002).

### 166 2.3. Cluster analysis

167 A daily meteorological analysis was undertaken based on 96-h isosigma back-trajectories at  
168 12:00h UTC and 1500m asl by using the HYSPLIT (Hybrid Single-Particle Lagrangian  
169 Integrated Trajectory) 4.0 dispersion model from the Air Resources Laboratory (ARL, available  
170 at <http://www.arl.noaa.gov/ready/hysplit4.html>, Draxler and Rolph 2003). This height can be  
171 taken as representative of the mean transport wind at a synoptic scale within the upper  
172 boundary layer. The meteorological input was obtained from the ARL (Air Resources Laboratory)  
173 reanalysis database for the 1984-1996 period, and from FNL for the 1997-2005 period and

174 from GDAS (Global Data Assimilation System) for 2006-2012, from the NCEP (National Center  
175 for Environmental Prediction). Even though the WeMO index corresponds to surface level  
176 pressures, a height of 1500 m, corresponding to 850 hPa standard pressure level, was selected  
177 for trajectory computation because both levels can be considered comparable for synoptic scale  
178 circulation features. Indeed, 850 hPa is the most representative level for transport in the lower  
179 troposphere. This layer is typically sensitive to cyclonic-wave features and is the approximate  
180 boundary between the surface-wind regime and the free troposphere (Artz et al. 1985).  
181 Moreover, a relationship between the 850 hPa wind direction and the prevailing weather  
182 patterns associated with the passage of cyclonic waves is well established (Dayan and Lamb  
183 2003).

184 Cluster analysis statistically aggregates observations into clusters so that each of them is as  
185 homogeneous as possible with respect to the clustering variables (Sharma 1996). To compose  
186 each cluster, HYSPLIT has a grouping module based on variations in the Total Spatial Variance  
187 (TSV) between different clusters which is compared to the spatial variance (SPVAR) within each  
188 cluster component. The final number of clusters is determined by a change in TSV as clusters  
189 are iteratively paired (Draxler et al. 2009). This statistical methodology was applied to daily  
190 trajectories for the period from 1984 to 2012. Because most of the variability patterns of the  
191 Northern Hemisphere show its most relevant dynamics during the winter (Goodess and Jones,  
192 2002; Martín-Vide and López-Bustins, 2006), a subset corresponding to the boreal winter period  
193 (December to March) was also analyzed.

194 The precipitation chemistry database consisted of weekly observations but trajectories were  
195 obtained daily. To overcome this mismatch we estimated a daily chemical concentration for the  
196 days with precipitation by proportionally correcting weekly chemical concentrations by the  
197 precipitation contribution of the rainy days to the weekly amount. The rainy days within each  
198 week and their precipitation amount were obtained from records at LC, and from the AEMET  
199 stations (Spanish Meteorological Service) of Turó de l'Home and Tagamanent which are 7 and  
200 8 Km distant from LC, respectively. Precipitation events of <3 mm were not included, and only  
201 the days with precipitation amount of >0.2 mm were considered for the determination of  
202 precipitation days within a week. The precipitation chemical concentrations were weighted by  
203 the precipitation amount to obtain ion volume weighted means (VWM, in  $\mu\text{eq L}^{-1}$ ). Wet  
204 deposition amounts ( $\text{kg ha}^{-1}\text{y}^{-1}$ ) were calculated as the product of VWM precipitation  
205 concentrations times the precipitation amount ( $\text{L m}^{-2}$ ).

206 We analyze here the atmospheric circulation patterns and the amount and chemistry of  
207 precipitation for:

208 1) An annual database, where the clustering methodology was applied to the daily trajectories  
209 for three periods encompassing a decade each: an early period (1984-1993), an  
210 intermediate period (1994-2003) and a recent one (2004-2012) period. This splitting was  
211 forced by the impossibility to deal with the whole dataset due to computing limitations. A

212 unique annual classification of air masses was obtained by combining the clusters of the  
213 three decades.

214 2) Winter database: Cluster analysis was applied to winter (DJFM) daily trajectories from 1984  
215 to 2012 in a single run.

216 The NAO (available at <https://climatedataguide.ucar.edu/climate-data/hurrell-north-atlantic-oscillation-nao-index-station-based>,  
217 Hurrell, James and National Center for Atmospheric  
218 Research Staff 2013) and WeMO (available at <http://www.ub.edu/gc/English/wemo.htm>, Group  
219 of Climatology, University of Barcelona) indexes for the annual and winter period (DJFM) were  
220 regressed (least-square linear regressions) with: 1) the frequency of provenances, 2) the  
221 number of rainy days in each provenance and 3) the amount of precipitation amount ( $L m^{-2}$ ) in  
222 each provenance from both (annual and winter) datasets. Regressions were also explored for  
223 these climatic indices (winter period) and winter wet deposition amount for the main  
224 precipitation components calculated for each provenance. The WeMOi value for 2012 was  
225 unavailable, therefore regressions considered the 1984-2011 period. In addition years 2001,  
226 2002, 2004 and 2005 were not included due to fragmentary precipitation chemistry sampling.  
227 Correlation coefficients of the regressions were considered significant when  $p < 0.05$ .

### 228 3. Results

#### 229 3.1. Annual atmospheric circulation patterns and precipitation regime

230 Back-trajectory clusters obtained from the annual database were classified in seven main  
231 provenances: 1) Northern flows, 2) North-Western, 3) Western, 4) North-Eastern, 5)  
232 Mediterranean, 6) Iberian Peninsula and 7) Regional/Local recirculation.

233 The annual NAOi was negatively correlated with Northern ( $R = -0.40$   $p < 0.05$ ) and positively with  
234 Mediterranean ( $R = 0.39$   $p < 0.05$ ) annual precipitation amount, but no correlation was found  
235 between annual NAOi and the frequency, the number of rainy days, and annual precipitation  
236 amounts of provenances other than the Mediterranean and Northern ones (Table 1). The  
237 annual WeMOi was positively correlated with the frequency and the number of rainy days of NW,  
238 W, Mediterranean and Regional provenances, and with the NW precipitation amount (Table 1).  
239 Conversely, annual WeMOi showed a negative significant relationship with Northern frequency  
240 and number of rainy days ( $R = -0.54$  and  $-0.35$ ; Table 1).

#### 241 3.2. Winter atmospheric routes and precipitation regime

242 The cluster analysis of winter (DJFM) daily trajectories from 1984 to 2012 showed seven main  
243 winter transport routes (Fig.2): Northern flows (cluster1), North-Western (cluster 2 and 3),  
244 Western (cluster 4 and 5), South-Western (cluster 6) and North-Eastern (cluster 7). Figure 2  
245 shows winter frequencies for each cluster. This classification broadly matched the annual one,  
246 except that the Iberian and Regional/Local clusters did not appear. Instead, a SW cluster was  
247 obtained.

248 The winter NAOi was negatively correlated with the number of rainy days and the precipitation  
249 amounts when considering all provenances together ( $R = -0.57$  and  $-0.48$  respectively; Table 2)

250 When split by clusters, winter NAOi showed negative correlations with frequency, number of  
251 rainy days and precipitation amount in the NW moderate cluster ( $R = -0.52$ ,  $-0.69$  and  $-0.68$ ;  
252  $p < 0.05$ ; Table 2). Also a negative significant correlation was observed for NAOi and  
253 precipitation amount in SW flows ( $R = -0.42$ ).

254 When considering all provenances together, the winter WeMOi was only significantly (and  
255 negatively) correlated with precipitation amount ( $R = -0.38$ ; Table 2). When split by clusters, the  
256 winter WeMOi was negatively correlated with the frequency and number of rainy days in SW  
257 and NE provenances; for the former one, also the precipitation amount was inversely correlated  
258 (Table 2). On the other hand, winter WeMOi was positively correlated with the provenance  
259 frequency and number of precipitation days in NW fast and W fast clusters (Table 2). These fast  
260 Atlantic trajectories accounted for 20% of total winter days while provenances from SW and NE  
261 about doubled this frequency (37%) and represented about 60% of winter precipitation amount  
262 (Fig. 2). The time trends of winter frequencies by cluster were also analysed. Frequencies of all  
263 clusters showed non-significant trends, except for the W fast cluster that showed a significant  
264 decreasing trend ( $R = -0.40$ ;  $p = 0.03$ ).

### 265 3.3. Winter precipitation deposition fluxes

266 Winter NAOi was inversely correlated with deposition fluxes of anthropogenic compounds ( $H^+$ ,  
267  $NH_4^+$ ,  $NO_3^-$  and  $SO_4^{2-}$ ) in W moderate flows (Table 4).

268 Winter WeMOi was negatively correlated with the winter deposition of marine ions ( $Na^+$ ,  $Mg^{2+}$   
269 and  $Cl^-$ ) and anthropogenic compounds ( $NH_4^+$ ,  $NO_3^-$  and  $SO_4^{2-}$ ) for the SW cluster (Table 4). On  
270 the other hand, a positive relationship was found between winter WeMOi and the deposition of  
271  $Ca^{2+}$ ,  $NH_4^+$ ,  $NO_3^-$  and  $SO_4^{2-}$  from W fast fluxes (Table 4). When considering the whole data  
272 irrespective of provenance distinction, only a negative correlation was found between WeMOi  
273 and  $NO_3^-$  (Table 4).

274 Winter SW deposition fluxes accounted for 28-34% of total winter deposition for all chemical  
275 compounds (Table 5). In fact SW plus NE deposition fluxes accounted for between 50% and  
276 65%, whereas W moderate and fast deposition fluxes only represented 9-17% and 5-10% of  
277 deposition respectively (Table 5).

## 278 4. Discussion

### 279 4.1. The influence of NAO and WeMO on the annual atmospheric circulation patterns and 280 precipitation amount

281 There is a general interest regarding the effects of the atmospheric dynamics, especially in a  
282 context of climate change. We analyzed the influence of NAO and WeMO on the atmospheric



283 transport routes and precipitation amount. The NAO is a large-scale oscillation in atmospheric  
284 mass, with centres of action near Iceland and over subtropical Atlantic (Visbeck et al. 2001).  
285 WeMO is a pattern of low-frequency variability defined as an alternative to the NAO for  
286 explaining the precipitation behavior on the East coast of the IP (Martín-Vide and Lopez-Bustins  
287 2006). Consequently, the use of the WeMOi is justified here by its clear influence on  
288 Mediterranean coastal precipitation (Gonzalez-Hidalgo et al. 2009), which is very weakly  
289 correlated to the NAO (Rodó et al. 1997).

290 Analysis of the data at an annual timeframe (Table 1) showed the lack of correlation between  
291 NAOi and the frequency of provenance, the number of rainy days and the precipitation amount,  
292 whereas WeMOi was significantly correlated with several of these variables. This indicated a  
293 stronger influence of WeMO in defining the precipitation in the Mediterranean coast (Table 1).  
294 Indeed, the positive correlations between WeMOi and Atlantic flows (NW and W provenances)  
295 was in accordance with what is expected in the WeMO positive phase (Martin-Vide and López-  
296 Bustins 2006; López-Bustins et al. 2008). However, the positive relationship between WeMOi  
297 and the Mediterranean provenance was unexpected considering the air fluxes, which head  
298 eastwards, in WeMO positive phase (Martin-Vide and López-Bustins 2006; López-Bustins et al.  
299 2008). Because of these contradictory results, cluster analysis was further explored for winter  
300 (December to March) since it is also the period where the influence of WeMO is most  
301 exacerbated in the Mediterranean coastal fringe (González-Hidalgo et al. 2009). Also the  
302 relationship between NAOi and precipitation is stronger in winter (Visbeck et al. 2001; Goodess  
303 and Jones 2002).

304 4.2. The influence of NAO and WeMO on the winter atmospheric transport routes and  
305 precipitation amount

306 Non significant correlations were observed between provenances and the positive NAO phase  
307 in winter (Table 2). In this mode, the pressure gradient between the Icelandic low and the  
308 subtropical high pressure centre is more intense than normal, so that westerly winds are  
309 stronger across northern Europe. This brings Atlantic air masses over the northern continent  
310 (associated with mild temperatures and higher precipitation) and dryer conditions across  
311 southern Europe. The negative relationship between NAO and the frequency and precipitation  
312 amounts from the W moderate cluster (Table 2) was in agreement with the fact that when the  
313 pressure gradient is low, cold and dry air masses often dominate over northern Europe and the  
314 Atlantic weather systems and storm tracks tend toward a more southerly trajectory, bringing  
315 higher than normal precipitation levels to the IP (Vicente-Serrano et al. 2011). The increase of  
316 total precipitation amount in the IP during negative winter NAO detected in previous studies  
317 (Goodess and Jones 2002; Rodríguez-Puebla and Nieto 2010; Vicente-Serrano et al. 2011),  
318 was also observed at LC.

319 In addition, results of the winter dataset showed that the changes in the frequency of  
320 circulations patterns were more closely associated to the influence of WeMO over the north-

321 eastern IP. The positive WeMO phase which corresponds to the anticyclone over the Azores  
322 enclosing the south-west Iberian quadrant and low-pressures in the Liguria Gulf (Martin-Vide  
323 and López-Bustins 2006) would agree with the occurrence of fast Atlantic flows. This was  
324 effectively observed for winter and for the whole year (Tables 2 and 3). The negative phase,  
325 which coincides with a central European anticyclone located north of the Italian peninsula and a  
326 low-pressure centre in the Iberian south-west (Martin-Vide and López-Bustins 2006) was well-  
327 correlated with the SW and NE clusters in winter. This corroborates that the most consistent  
328 results and the best correlations for circulation patterns were found during the winter period, as  
329 expected.

330 The decreasing trend of winter W fast cluster frequency and the low winter fast Atlantic  
331 frequencies observed (9%, Table 3) could be related with a major frequency of high pressures  
332 over Iberia at the end of 20<sup>th</sup> century, which prevents the arrival of Atlantic storms to  
333 Mediterranean latitudes. In fact, this could be the main cause of a significant decrease in winter  
334 precipitation registered in western and central IP, while no variations or even slight precipitation  
335 increase are detected on the eastern fringe as some north-easterly winds convey moisture to  
336 the south-eastern region (Lopez-Bustins et al. 2008). A non-significant time trend was observed  
337 for rainy days and precipitation amount in winter at LC, therefore no changes in winter  
338 precipitation behaviour were detected. Conversely, other studies showed an increase of the  
339 winter precipitation amount (Gonzalez-Hidalgo et al. 2009) as well as the torrential precipitation  
340 episodes (Goodess and Jones 2002; Martín-Vide et al. 2008) in the Mediterranean fringe of the  
341 IP.

342 The negative correlation (Table 2) between total winter precipitation amount at LC and the  
343 winter WeMO<sub>i</sub> indicates that higher precipitation amounts were registered from the  
344 Mediterranean than from the Atlantic provenance. This is consistent with the negative  
345 correlation between winter SW precipitation amount and the winter WeMO<sub>i</sub> at Montseny and  
346 that reported by other studies on the role of WeMO on precipitation in the eastern IP (Martín-  
347 Vide and López-Bustins, 2006; González-Hidalgo et al. 2009). It is important to note the high  
348 occurrence of rainy days from SW and NE flows, which accounted for 44% compared to 19%  
349 from fast Atlantic air masses. Both clusters represented ~ 60% of winter precipitation amount,  
350 indicating the dominant role of the negative WeMO phases in precipitation. The high SW and  
351 NE precipitation amounts (Table 3) may be related with the significant correlation between  
352 negative values of WeMO<sub>i</sub> and torrential precipitation in north-eastern IP, despite that,  
353 according to Martín-Vide et al. (2008), only 22% of torrential precipitation cases occurred in  
354 winter.

#### 355 4.3. The influence of winter WeMO<sub>i</sub> and NAO<sub>i</sub> on deposition fluxes

356 In Europe, the effects of NAO on air temperature, storminess and winds have been thoroughly  
357 studied (Hurrell and Deser 2010, and references therein), but very few studies have approached  
358 the links between the NAO variability and the chemistry of precipitation and wet deposition. One

359 exception to this are the works of Evans et al. (2001) and Fowler et al. (2005) for the British  
360 Islands. The former study took into account the winter NAO variability to interpret the variation  
361 of lake concentrations in the UK and concluded that a cycle of high deposition of marine ions in  
362 the early 1990s was in phase with the winter NAO indices and suggested the need for a further  
363 exploration of this relationship (Evans et al. 2001). Fowler et al. (2005) studied the effect of  
364 annual and winter NAO indices on wet deposition in the UK, but did not find significant  
365 relationships for any of the studied ions ( $\text{Na}^+$ ,  $\text{Cl}^-$ ,  $\text{NH}_4^+$ ,  $\text{NO}_3^-$ ,  $\text{SO}_4^{2-}$ ,  $\text{H}^+$ ); thus the NAO  
366 variability appeared to have a negligible effect for acidifying components regarding the changes  
367 in emissions in the UK.

368 Other studies have investigated the effect of NAO on atmospheric mineral dust and  
369 anthropogenic aerosols in the Mediterranean, and have found a correspondence between  
370 African particulate matter and NAO, particularly when considering the summer period (Moulin et  
371 al. 1997; Ginoux et al. 2004; Pey et al. 2013). However, wet deposition of dissolved African  
372 dusts did not show significant relationships with NAO in NE Spain (Àvila and Rodà, 2002). This  
373 was interpreted as resulting from two effects that vary in opposite directions: high NAO indices  
374 correspond to an increase of atmospheric dust (Cusack et al. 2012) but in years of high NAO  
375 there is a decrease in the precipitation amount in the IP, two processes that cancel each other  
376 in providing the deposition amounts (the product of concentrations times precipitation amount).

377 In Montseny, winter precipitation amount (Table 2) and deposition (Table 4) of  $\text{NO}_3^-$  were  
378 negatively correlated with winter WeMOi, indicating that the Catalan fringe receives higher  
379 precipitation and  $\text{NO}_3^-$ -N deposition when WeMO is in its negative phase during winter. The  
380 relationships between the trajectory frequencies and precipitation parameters with the studied  
381 indices were weak or counterintuitive in the annual dataset. The winter dataset produced more  
382 consistent results. However, for the NAO teleconnection, no significant relationships were found  
383 between the NAOi and the analysed precipitation variables and, for ion deposition, only when  
384 decomposing the data for provenances, a significant inverse relationship appeared with  
385 anthropogenic ions for the Western (moderate) provenance (Table 4). Several studies in the  
386 Iberian Peninsula have shown that the influence of NAOi is lower than the indices describing the  
387 Mediterranean variability such as the WeMOi or the MOi (Mediterranean Oscillation index)  
388 either at the annual scale (González Hidalgo et al. 2009) or specifically for winter (López-  
389 Bustins et al. 2008; González Hidalgo et al. 2009).

390 When decomposed by provenances, winter WeMOi showed negative correlations with the  
391 deposition of marine ions ( $\text{Na}^+$ ,  $\text{Mg}^{2+}$  and  $\text{Cl}^-$ ) and anthropogenic species ( $\text{NH}_4^+$ ,  $\text{NO}_3^-$  and  $\text{SO}_4^{2-}$ )  
392 in SW fluxes (Table 4). This implies that, during years characterized by negative winter WeMOi,  
393 SW air masses would convey higher deposition of the mentioned ions. Since the WeMO  
394 negative phase is associated to flows from the Mediterranean (Martin-Vide and López-Bustins  
395 2006; López-Bustins et al. 2008), a higher deposition of marine ions with negative WeMOi is an  
396 expected result. However, for  $\text{NO}_3^-$ ,  $\text{NH}_4^+$  and  $\text{SO}_4^{2-}$ , which are emitted mostly from continental

397 traffic, power generation, industrial activities and agriculture, this result suggests the presence  
398 over the Mediterranean of polluted air masses that would have been advected from highly  
399 industrialised areas in southern Europe, and then they will be delivered by Mediterranean  
400 precipitation events. In fact, Millán et al. (1997) have described a recirculation process of air  
401 masses that occurs over the Western Mediterranean and favours the accumulation of  
402 atmospheric anthropogenic pollutants across the area. These pollutants are probably  
403 incorporated into the precipitation during negative WeMO phases producing the observed  
404 enhanced deposition observed for  $\text{NH}_4^+$ ,  $\text{NO}_3^-$  and  $\text{SO}_4^{2-}$ . The study of more anthropogenic-  
405 derived components in the precipitation (e.g. trace metals) could help validate this statement.  
406 On the other hand, the growing industrialisation in North Africa and the intensification of ship  
407 traffic on the Mediterranean has also been suggested contribute to anthropogenic deposition  
408 associated with Mediterranean provenances (Izquierdo et al. 2012).

409 In Table 4 it is seen that the NAOi has a negative significant correlation with anthropogenic  
410 pollutants but only in the West moderate cluster. Thus it is seen that both indices explain  
411 different parts of the variation, with the WeMOi influencing SW and W fast flows and the NAO  
412 influencing Western flows of shorter spatial range.

413 Furthermore, local emissions may also have a role. Especially, extremely intense pollution  
414 episodes associated with the transport by sea-mountain breezes of aged air masses from  
415 industrial/urban areas around major cities such as Barcelona during winter anticyclonic  
416 episodes (WAE) (Pérez et al. 2008; Pey et al. 2010). Usually, the meteorological conditions  
417 during these episodes enhance the local anthropogenic resuspension processes in urban areas,  
418 but also favour the transport of aerosols to nearby mountains such as Montseny. These specific  
419 features and the intense emissions of ammonia in the northeastern IP give rise to the formation  
420 of high amounts of secondary inorganic aerosols, mainly ammonium nitrate, and in minor  
421 proportion ammonium sulphate, recorded at LC during these meteorological scenarios (Pey et  
422 al. 2010). At the end of the WAE, stagnant polluted air masses are replaced by air masses  
423 coming from Mediterranean or Atlantic (Pey et al. 2010). As Mediterranean episodes are related  
424 with the occurrence of precipitation (Pérez et al. 2008),  $\text{NH}_4^+$ ,  $\text{NO}_3^-$ , and  $\text{SO}_4^{2-}$  from local  
425 anthropogenic emissions may be incorporated into precipitation and contribute to the correlation  
426 with the WeMOi. The WAE in wintertime was recurrent with a mean frequency from 15% to 25%  
427 of the days (Cusack et al. 2012).

428 A positive correlation was observed between winter WeMOi and the deposition of  $\text{Ca}^{2+}$ ,  $\text{NH}_4^+$ ,  
429  $\text{NO}_3^-$  and  $\text{SO}_4^{2-}$  in W fast fluxes, indicating higher deposition of the mentioned ions associated to  
430 the positive phase of WeMO. This is consistent with the description of the WeMO positive phase  
431 as triggering air fluxes from the Atlantic into the IP (Martin-Vide and López-Bustins 2006) that  
432 would arrive to the Mediterranean coast. Previous studies showed that Atlantic advection  
433 episodes could have a cleaning effect on aerosols at LC (Cusack et al. 2012), therefore the  
434 winter WeMOi relationship with the anthropogenic-derived species may be attributed to WAE as

435 has been explained above. However, this provenance only contributed to 9% (Table 3) of total  
436 precipitation at our site, compared to the SW provenance which accounted for 33% total  
437 precipitation. In terms of deposition, the SW provenance accounted for 29%, 28% and 32% of  
438  $\text{NO}_3^-$ -N,  $\text{NH}_4^+$ -N and  $\text{SO}_4^{2-}$ -S fluxes (Table 5) compared to 7%, 10% and 8%, of  $\text{NO}_3^-$ -N,  $\text{NH}_4^+$ -N  
439 and  $\text{SO}_4^{2-}$ -S fluxes for the fast West provenance. This suggests that most of the anthropogenic  
440 pollutants deposited at Montseny can be attributed to the arrival of Mediterranean air masses.  
441 Thus the WeMO index, which in its negative phase triggers the transport of air masses from the  
442 Mediterranean to the Iberian Peninsula, can be partially used to describe the precipitation  
443 amounts and the anthropogenic pollutant deposition variability at the northeast fringe of the  
444 Iberian Peninsula.

## 445 5. Conclusions

446 This study has shown that the influence of the NAO index is lower than an index describing the  
447 Mediterranean variability, the WeMOi, at a site in the northeast of the Iberian Peninsula.  
448 Consistently with other works in the west Mediterranean, winter precipitation amount was  
449 inversely correlated with winter WeMOi and NAOi. The relationship between element deposition  
450 and indices of climatic variability has not been usually explored in the literature for Europe, other  
451 than a few studies in the British Isles in which the NAO variability had a negligible effect for  
452 acidifying components albeit a probable influence for marine ions.

453 Our results indicated the relevant role of the WeMO and the NAO in the deposition of  
454 anthropogenic pollutants ( $\text{H}^+$ ,  $\text{NH}_4^+$ ,  $\text{NO}_3^-$  and  $\text{SO}_4^{2-}$ ). For marine ions ( $\text{Cl}^-$ ,  $\text{Na}^+$ ,  $\text{Mg}^{2+}$ ) only the  
455 WeMOi had a significant effect. The cluster classification of provenances indicated that fast  
456 Atlantic air flows corresponded to positive winter WeMO indices, while negative winter WeMOi  
457 were associated to NE and SW circulations in winter. Most of the ion deposition was conveyed  
458 by air masses from the Mediterranean and was significantly correlated with the negative phase  
459 of the WeMO. These Mediterranean episodes can bring pollution from aged air masses  
460 recirculated in the Western Mediterranean and also incorporate local anthropogenic emissions  
461 from winter anticyclonic episodes.

## 462 Acknowledgements

463 We acknowledge the financial support from the Spanish Government (CGL2012-39523-C02-02,  
464 CGL2009-13188-C03-01, CGL2009-11205, CSD2008-00040-Consolider Montes and CSD  
465 2007-00067-Consolider GRACCIE). Javier Martín-Vide and Joan Albert López-Bustins from the  
466 Group of Climatology (University of Barcelona) are thanked for WeMOi data, and Mirna Lopez  
467 for assistance with back-trajectory analysis.

468

469

470

471 References

472 Artz, R., Pielke, R.A., Galloway, J. 1985. Comparison of the ARL/ATAD constant level and the  
473 NCAR isentropic trajectory analyses for selected case studies. *Atmospheric Environment* 19,  
474 47-63

475 Àvila, A. 1996. Time trends in the precipitation chemistry at a mountain site in Northeastern  
476 Spain for the period 1983-1994. *Atmospheric Environment* 30, 1363-1373.

477 Àvila, A., Queralt-Mitjans, I., Alarcón, M. 1997. Mineralogical composition of African dust  
478 delivered by red rains over north-eastern Spain. *Journal of Geophysical Research D18*, 21977-  
479 21996.

480 Àvila, A., Alarcón, M. 1999. Relationship between precipitation chemistry and meteorological  
481 situations at a rural site in NE Spain. *Atmospheric Environment* 33, 1663-1677.

482 Àvila, A., Rodà, F. 2002. Assessing decadal changes in rainwater alkalinity at a rural  
483 Mediterranean site in the Montseny Mountains (NE Spain). *Atmospheric Environment* 36, 2881-  
484 2890.

485 Àvila, A., Alarcón, M. 2003. Precipitation chemistry at a rural mediterranean site: between  
486 anthropogenic pollution and natural emissions. *Journal of Geophysical Research-Atmospheres*  
487 108, D9, 4278.

488 Àvila, A., Alarcón, M., Castillo, S., Escudero, M., García-Orellana, J., Masqué, P. Querol, X.  
489 2007. Variation of soluble and insoluble calcium in red-rains related to dust sources and  
490 transport patterns from North Africa to northeastern Spain. *Journal of Geophysical Research*  
491 112, D05210.

492 Barkhordarian, A., von Storch, H., Bhend, J. 2013. The expectation of future precipitation  
493 change over the Mediterranean region is different from what we observe. *Climate Dynamics* 40,  
494 225-244.

495 Carnell, RE., Senior, CA. 2002. An investigation into the mechanisms of changes in mid-latitude  
496 mean sea level pressure as greenhouse are increased. *Climate Dynamics* 18, 533-543.

497 Cusack, M., Alastuey, A., Pérez, N., Pey, J., Querol, X. 2012. Trends of particulate matter  
498 (PM<sub>2.5</sub>) and chemical composition at a regional background site in the Western Mediterranean  
499 over the last nine years (2002-2010). *Atmospheric Chemistry and Physics* 12, 8341-8357.

500 Dayan, U., Lamb, D. 2003. Meteorological indicators of summer precipitation chemistry in  
501 central Pennsylvania. *Atmospheric Environment* 37, 1045-1055.

502 Draxler, R.R., Rolph, G.D. 2003. HYSPLIT (HYbrid Single-Particle Lagrangian Integrated  
503 Trajectory) Model access via NOAA ARL READY website ([http://www.arl.noaa.gov/ready](http://www.arl.noaa.gov/ready/hysplit4.html)  
504 [/hysplit4.html](http://www.arl.noaa.gov/ready/hysplit4.html)). NOAA Air Resources Laboratory, Silver Spring, MD.

505 Draxler, R.R., Stunder, B., Rolph, G., & Taylor, A. 2009. HYSPLIT\_4 User's Guide. NOAA Air  
506 Resources Laboratory ([http://www.arl.noaa.gov/documents/reports/hysplit\\_user\\_guide.pdf](http://www.arl.noaa.gov/documents/reports/hysplit_user_guide.pdf)).

507 Escudero, M., Castillo, S., Querol, X., Àvila, A., Alarcón, M., Viana, M.M., Alastuey, A., Cuevas,  
508 E., Rodríguez, S. 2005. Wet and dry African dust episodes over eastern Spain. *Journal of*  
509 *Geophysical Research* 110, D18S08.

510 Escudero, M., Querol, X., Àvila, A., Cuevas, E. 2007. Origin of the exceedances of the  
511 European daily PM limit value in regional background areas of Spain. *Atmospheric Environment*  
512 41, 730–744.

513 Escudero, M., Stein, AF., Draxler, RR., Querol, X., Alastuey, A., Castillo, S., Àvila, A. 2011.  
514 Source apportionment for African dust outbreaks over the Western Mediterranean using the  
515 HYSPLIT model. *Atmospheric Research* 99 (3-4), 518-527.

516 Evans CD., Monteith DT., Harriman R. 2001. Long-term variability in the deposition of marine  
517 ions at west coast sites in the UK Acid Waters Monitoring Network: impacts on surface water  
518 chemistry and significance for trend determination. *The Science of Total Environment* 265, 115-  
519 129.

520 Fowler, D., Smith RI., Muller, JBA., Hayman, G., Vincent KJ. 2005. Changes in the atmospheric  
521 deposition of acidifying compounds in the UK between 1986 and 2001. *Environmental Pollution*  
522 137, 15-25.

523 Gillett, NP., Allen, MR., McDonald, RE., Senior, CA., Shindell, DT., Schmidt, GA. 2005. How  
524 linear is the Arctic Oscillation response to greenhouse gases? *Journal of Geophysical*  
525 *Research-Atmospheres* 107, D3, 4022.

526 Gionux, P., Prospero, J.M., Torres, O., Chin, M. 2004. Long-term simulation of global dust with  
527 the GOCART model: correlation with North Atlantic Oscillation. *Environmental Modelling and*  
528 *Software*. 19, 113-128.

529 Gonzalez-Hidalgo, J.C., Lopez-Bustins, J.A., Štěpánek, P., Martin-Vide, J., de Luis, M. 2009.  
530 Monthly precipitation trends on the Mediterranean fringe of the Iberian Peninsula during the  
531 second-half of the twentieth century (1951-2000). *International Journal of Climatology* 29, 1415-  
532 1429.

533 Goodess, CM., Jones, PD. 2002. Links between circulation and changes in the characteristics  
534 of Iberian rainfall. *International Journal of Climatology* 22, 1593-1615.

535 Hurrell, JW. 1995. Decadal trend in the North-Atlantic oscillation – regional temperatures and  
536 precipitation. *Science* 269, 676-679.

537 Hurrell, JW., Hoerling, MP., Phillips, AS., Xu, T. 2004. Twentieth century north atlantic climate  
538 change. Part I: assessing determinism. *Climate Dynamics* 23, 371-389.

539 Hurrell, JW., Deser, C. 2010. North Atlantic climate variability: The role of the North Atlantic  
540 Oscillation. *Journal of Marine Systems* 79, 231-244.

541 Hurrell, James & National Center for Atmospheric Research Staff (Eds). Last modified 08 Oct  
542 2013. "The Climate Data Guide: Hurrell North Atlantic Oscillation (NAO) Index (station-based)."  
543 Retrieved from [https://climatedataguide.ucar.edu/climate-data/hurrell-north-atlantic-oscillation-](https://climatedataguide.ucar.edu/climate-data/hurrell-north-atlantic-oscillation-nao-index-station-based)  
544 [nao-index-station-based](https://climatedataguide.ucar.edu/climate-data/hurrell-north-atlantic-oscillation-nao-index-station-based).

545 IPCC, 2007. *Climate Change 2007. The Physical Science Basis*. In: Solomon, S., Qin, D.,  
546 Manning, M., Chen, Z., Marquis, M., Averyt, K.B., Tignor, M., Miller, H.L. (Eds.), *Contribution of*  
547 *Working Group I to the Fourth Assessment Report of the Intergovernmental Panel on Climate*  
548 *Change*. Cambridge University Press, Cambridge, United Kingdom and New York, NY, USA.  
549 996 pp.

550 Izquierdo R., Àvila A. 2012. Comparison of collection methods to determine atmospheric  
551 deposition in a rural Mediterranean site (NE Spain), *Journal of Atmospheric Chemistry* 69, 351-  
552 368.

553 Izquierdo, R., Àvila, A., Alarcón, M. 2012. Trajectory statistical analysis of atmospheric transport  
554 patterns and trends in precipitation chemistry of a rural site in NE Spain in 1984-2009,  
555 *Atmospheric Environment* 61, 400-408.

556 Lionello, P., Malanotte-Rizzoli, P., Boscolo, R., Alpert, P., Artale, V. Li, L., Luterbacher, J., May,  
557 W., Trigo, R., Tsimplis, M., Ulbrich, U., Xoplaki, E. 2006. The Mediterranean climate; an  
558 overview of the main characteristics and issues. In: Lionello, P., Malanotte-Rizzoli, P. Boscolo,  
559 R. (eds). *Mediterranean climate variability*. *Developments in Earth and Environmental Sciences*  
560 4, Elsevier, Amsterdam.

561 Lopez-Bustins, J.A., Martín-Vide, J., Sanchez-Lorenzo, A. 2008. Iberia Winter rainfall trends  
562 based upon changes in teleconnection and circulation patterns. *Global and Planetary Change*  
563 63, 171-176.

564 Mariotti, A., Dell' Aquila, A. 2012. Decadal climate variability in the Mediterranean region: roles  
565 of large-scale forcings and regional processes. *Climate Dynamics* 38, 1129–1145.



566 Martín-Vide, J., Lopez-Bustins, J.A. 2006. The Western Mediterranean Oscillation and rainfall in  
567 the Iberian Peninsula, *International Journal of Climatology*. 26 (11), 1455-1475. Website:  
568 <http://www.ub.edu/gc/English/wemo.htm>

569 Martín-Vide, J., Sanchez-Lorenzo, A., Lopez-Bustins, J.A., Cordobilla, M.J., Garcia-Manuel, A.,  
570 Raso, J.M. 2008. Torrential rainfall in northeast of the Iberian Peninsula: synoptic patterns and  
571 WeMO influence. *Advances in Science and Research* 2, 99-105.

572 Matthias, V., Bewersdorff, I., Aulinger, A., Quante, M. 2010. The contribution of ship emissions  
573 to air pollution in the North Sea regions. *Environmental Pollution* 158, 2241-2250.

574 Millán, M.M., Artífano, B., Alonso, L.A., Navazo, M., Castro, M. 1991. The effect of meso-scale  
575 flows on regional and long-range atmospheric transport in the Western Mediterranean area.  
576 *Atmospheric Environment* 25, 949-963.

577 Millán M., Salvador R., Mantilla E., Kallos G. 1997. Photo-oxidant dynamics in the  
578 Mediterranean basin in summer: results from European research projects. *Journal of*  
579 *Geophysical Research* 102, 8811-8823.

580 Min, SK.; Zhang, XB.; Zwiers, FW., Hegerl, GC. 2011. Human contribution to more-intense  
581 precipitation extremes. *Nature* 470, 376-379.

582 Morales-Baquero, R., Pulido-Villena, E., Reche, I. 2013. Chemical signature of Saharan dust on  
583 dry and wet atmospheric deposition in the south-western Mediterranean region. *Tellus series B-*  
584 *Chemical and Physical Meteorology* 65, 18720.

585 Moulin, C., Lambert, C.E., Dulac, F., Dayan, U. 1997. Control of atmospheric export of dust from  
586 North Africa by the North Atlantic Oscillation. *Nature* 387, 691-694.

587 Pérez, N., Pey, J., Castillo, S., Viana, M.M., Alastuey, A., Querol, X. 2008. Interpretation of the  
588 variability of levels of regional background aerosols in the Western Mediterranean. *Science of*  
589 *the Total Environment* 407, 527-540.

590 Pey, J., Pérez, N., Castillo, S., Viana, M., Moreno, T., Pandolfi, M., López-Sebastián, J.M.,  
591 Alastuey, A., Querol, X. 2009. Geochemistry of regional background aerosols in the Western  
592 Mediterranean. *Atmospheric Research* 94, 422-435.

593 Pey, J., Pérez, N., Querol, X., Alastuey, A., Cusack, M., Reche, C. 2010. Intense Winter  
594 atmospheric pollution episodes affecting the Western Mediterranean. *Science of the Total*  
595 *Environment* 408, 1951-1959.

596 Pey, J., Querol, X., Alastuey, A., Forastiere, F., Stafoggia M. 2013. African dust outbreaks over  
597 the Mediterranean Basin during 2001-2011: PM10 concentrations, phenomenology and trends,

598 and its relation with synoptic and mesoscale meteorology. *Atmospheric Chemistry and Physics*  
599 13, 1395-1410.

600 Pulido-Villena, E., Reche, I. and Morales-Baquero, R. 2006. Significance of atmospheric inputs  
601 of calcium over the southwestern Mediterranean region: high mountain lakes as tools for  
602 detection. *Global Biogeochemical Cycles* 20, GB2012.

603 Querol, X., Pey, J., Pandolfi, M., Alastuey, A., Cusack, M., Pérez, N., Moreno, T., Viana, M.M.,  
604 Mihalopoulos, M., Kallos, G., Kleanthous, S. 2009. African dust contributions to mean ambient  
605 PM10 mass-levels across the Mediterranean Basin. *Atmospheric Environment* 43, 4266-4275.

606 Rodó X, Baert E, Comin FA. 1997. Variations in seasonal rainfall in Southern Europe during the  
607 present century: relationships with the North Atlantic Oscillation and the El Niño-Southern  
608 Oscillation. *Climate Dynamics* 13, 275–284.

609 Rodà, F., Retana, J., Gracia, C.A., Bellot, J. 1999 Ecology of Mediterranean Evergreen Oak  
610 Forests. *Ecological Studies* 137 (373pp). Springer. Berlin.

611 Rodríguez, S., Querol, X., Alastuey, A., Mantilla, E. 2003. Events affecting levels and seasonal  
612 evolution of airborne particulate matter concentrations in the Western Mediterranean.  
613 *Environmental Science and Technology* 37, 216-222.

614 Rodríguez-Puebla, C., Nieto, S. 2010. Trends of precipitation over the Iberian Peninsula and the  
615 North Atlantic Oscillation under climate change. *International Journal of Climatology* 30, 1807-  
616 1815.

617 Sharma, S. 1996. *Applied Multivariate Techniques*. John Wiley & Sons, Inc. New York, pp.493

618 Vicente-Serrano, SM., Trigo, RM., López-Moreno, JI., Liberato MLR., Lorenzo-Lacruz, J.,  
619 Beguería, S., Morán-Tejeda, E. 2011. Extreme winter precipitation in the Iberian Peninsula in  
620 2010: anomalies, driving mechanisms and future projections. *Climate Research* 46, 51-65.

621 Visbeck, MH., Hurrell, JW., Polvani, L., Cullen, HM. 2001. The North Atlantic Oscillation: past,  
622 present and future. *Proceedings of the National Academy of Sciences of the United States of*  
623 *America* 98, 12876-12877.

624 Wallace, J.M. 2000. North Atlantic Oscillation/annular mode: two paradigms – one phenomenon.  
625 *Quarterly Journal of the Royal Meteorological Society* 126, 791-805.

626 Xoplaki, E., Gonzalez-Rouco, JF., Luterbacher, J., Wanner, H. 2004. Wet season  
627 Mediterranean precipitation variability: influence of large-scale dynamics and trends. *Climate*  
628 *Dynamics* 23, 63-78.

629 Zhang, X., Zwiers, FW., Hegerl, CH., Lambert, FH., Gillett, NP., Solomon, S., Stott, PA.,  
630 Nozawa, T. 2007. Detection of human influence on twentieth-century precipitation trends.  
631 Nature 448, 461-465.

632

633

Author's accepted manuscript

634 TABLES

635 Table 1. Annual dataset: significant correlation coefficients ( $p < 0.05$ ) between the studied  
 636 climatic variability indices (NAOi and WeMOi) and the provenance frequency, number of rainy  
 637 days and the precipitation amount distinguished by provenances from the cluster analysis, for  
 638 the period 1984-2012.

Annual provenances	Provenance frequency (%)		Number of rainy days		Precipitation amount (mm)	
	NAOi	WeMOi	NAOi	WeMOi	NAOi	WeMOi
1. N		-0.54		-0.35	-0.40	
2. NW		0.63		0.46		0.41
3. W		0.49		0.35		
4. NE						
5. MED		0.49		0.46	0.39	
6. IP						
7. REG		0.52		0.59		
TOTAL						

639

640

Author's accepted manuscript

641

642 Table 2. Winter (DJFM) dataset: significant correlation coefficients ( $p < 0.05$ ) between the studied  
643 climatic variability indices (NAOi and WeMOi) and the provenance frequency, number of rainy  
644 days and the precipitation amount distinguished by provenances from the cluster analysis for  
645 the period 1984-2012.

Winter provenances	Provenance frequency (%)		n rainy days		Precipitation amount (mm)	
	NAOi	WeMOi	NAOi	WeMOi	NAOi	WeMOi
C1.N fast						
C2. NW fast		0.59		0.45		
C3. NW slow						
C4. W fast		0.69		0.48		
C5.W moderate	-0.52		-0.69		-0.68	
C6. SW		-0.57		-0.59	-0.42	-0.58
C7. NE		-0.66	-0.39	-0.60		
Total			-0.57		-0.48	-0.38

646

647

Author's accepted manuscript

648 Table 3.. Frequency of rainy days and precipitation amount for each cluster in winter (DJFM)  
 649 from 1984 to 2012.

	n rainy days	Rainy days vs. total rainy days	Precipitation amount (mm)	% Total precipitation amount
C1.N fast	69	7%	145	2%
C2. NW fast	82	8%	332	5%
C3. NW slow	155	15%	878	12%
C4. W fast	107	11%	649	9%
C5.W moderate	152	15%	976	13%
C6. SW	208	21%	2405	33%
C7. NE	238	23%	1928	26%
Total	1011	100%	7313	100%

650

651

652

Author's accepted manuscript

653

654 Table 4. Significant correlation coefficients ( $p < 0.05$ ) between winter (DJFM) NAOi/WeMOi and winter ion deposition in precipitation for each cluster in the  
 655 1984-2012 period.

656

Winter deposition	Winter NAOi							Winter WeMOi						
	H <sup>+</sup>	Na <sup>+</sup> /Cl <sup>-</sup>	Mg <sup>2+</sup>	Ca <sup>2+</sup>	NH <sub>4</sub> <sup>+</sup>	NO <sub>3</sub> <sup>-</sup>	SO <sub>4</sub> <sup>2-</sup>	H <sup>+</sup>	Na <sup>+</sup> /Cl <sup>-</sup>	Mg <sup>2+</sup>	Ca <sup>2+</sup>	NH <sub>4</sub> <sup>+</sup>	NO <sub>3</sub> <sup>-</sup>	SO <sub>4</sub> <sup>2-</sup>
C1.N fast														
C2. NW fast														
C3. NW slow														
C4. W fast											0.45	0.52	0.43	0.55
C5.W moderate	-0.46				-0.54	-0.46	-0.46							
C6. SW									-0.47/-0.45	-0.48		-0.50	-0.67	-0.42
C7. NE														
Total													-0.45	

657

658

659 Table 5. Winter element deposition (in kg ha<sup>-1</sup> y<sup>-1</sup>) for each cluster and the percentage accounted by each one for the period 1984-2012.

Winter ion deposition (DJFM)	C1.N fast	C2. NW fast	C3. NW slow	C4. W fast	C5.W moderate	C6. SW	C7. NE	Total
Na <sup>+</sup>	0.019 1.2%	0.064 3.9%	0.180 11.1%	0.120 7.3%	0.171 10.5%	0.556 34.2%	0.518 31.8%	1.63 100%
Ca <sup>2+</sup>	0.031 1.5%	0.088 4.2%	0.213 10.1%	0.098 4.7%	0.353 16.8%	0.709 33.7%	0.610 29.0%	2.10 100%
Mg <sup>2+</sup>	0.004 1.6%	0.011 4.2%	0.033 12.3%	0.022 8.0%	0.031 11.3%	0.088 32.3%	0.082 30.3%	0.272 100%
NH <sub>4</sub> <sup>+</sup> -N	0.015 2.5%	0.056 9.0%	0.082 13.2%	0.062 10.0%	0.086 13.8%	0.177 28.3%	0.146 23.3%	0.626 100%
NO <sub>3</sub> <sup>-</sup> -N	0.017 2.6%	0.044 6.8%	0.091 14.1%	0.048 7.4%	0.085 13.2%	0.190 29.4%	0.170 26.4%	0.645 100%
SO <sub>4</sub> <sup>2-</sup> -S	0.022 1.8%	0.070 5.5%	0.163 13.0%	0.094 7.5%	0.150 12.0%	0.398 31.7%	0.358 28.5%	1.26 100%
Cl <sup>-</sup>	0.035 1.2%	0.121 4.0%	0.344 11.3%	0.236 7.7%	0.330 10.8%	1.03 33.7%	0.959 31.4%	3.05 100%
H <sup>+</sup>	0.0006 1.9%	0.0009 3.0%	0.005 16.7%	0.002 7.0%	0.003 8.6%	0.011 34.5%	0.009 28.4%	0.031 100%

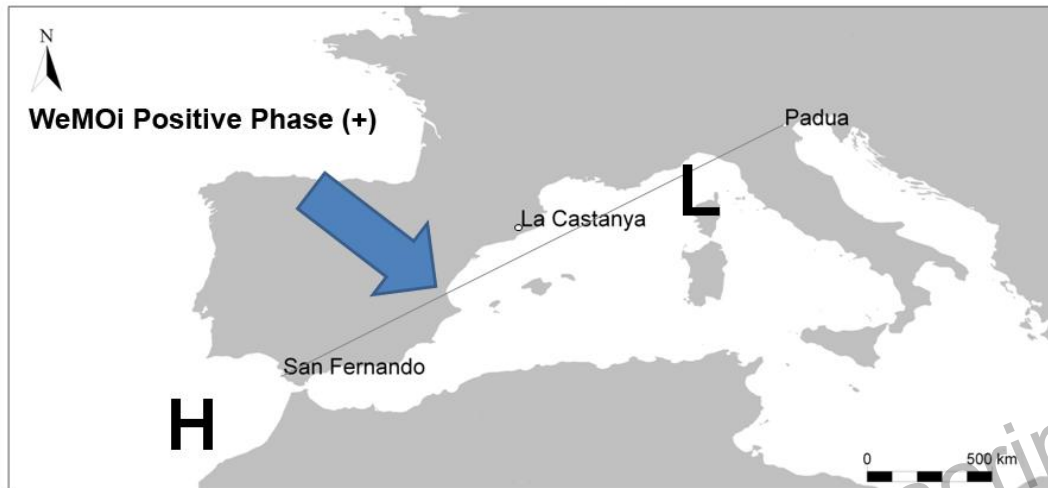
660



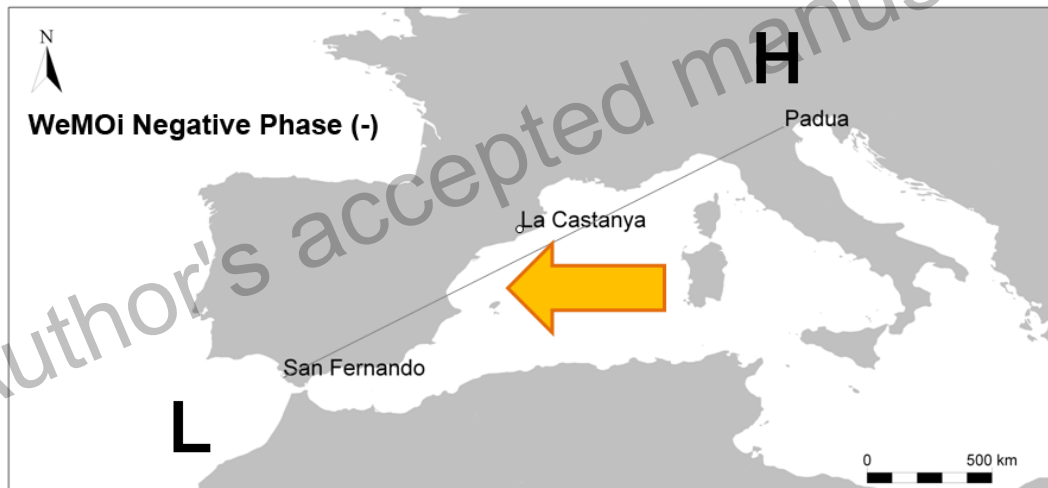
661 FIGURES

662 Figure 1. Location of La Castanya study site (LC) and WeMO phases

663



664



665

666

667

668

669

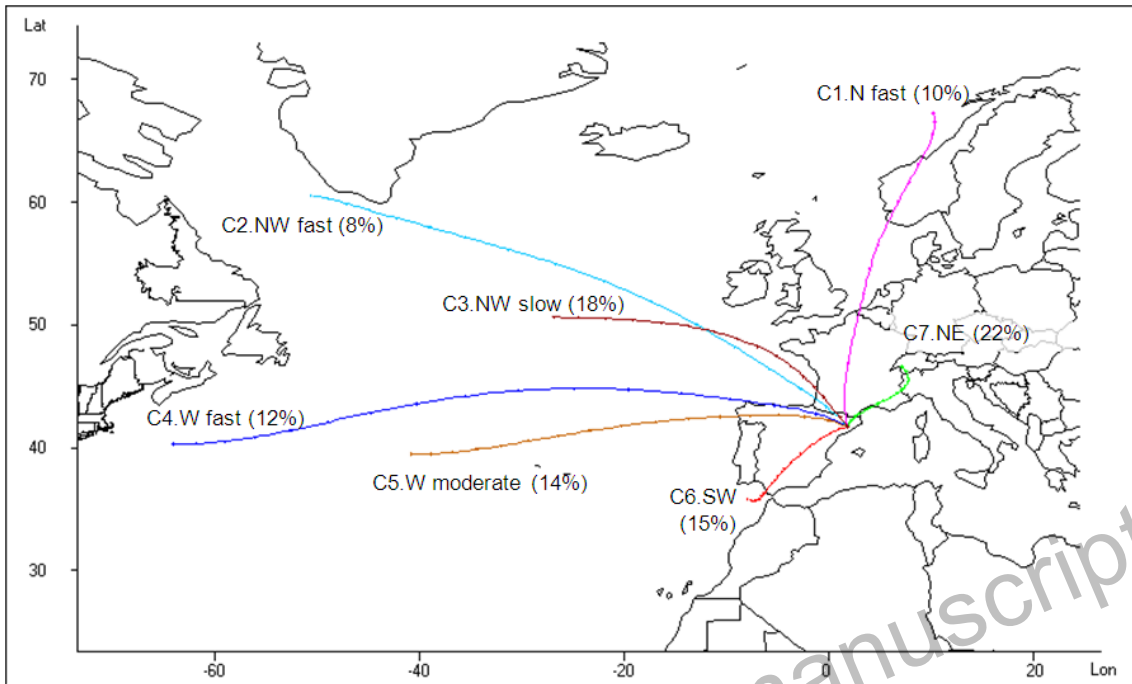
670

671

672

673 Figure 2. Back-trajectory centroids and frequency associated to each cluster in winter (DJFM)  
674 for 1984-2012 periods. Back-trajectories (72h) from LC calculated at 1500m asl.

675



676